SUMMARY

The seismicity recorded in El Salvador is generated for two principal sources: The subduction process of the Cocos plate under the Caribbean plate and local fault movements or volcanic activity. The destructive earthquakes in El Salvador has been located in the volcanic chain. In the present work the seismictity located along the volcanic chain by CIG (Centro de Investigaciones Geotécnicas) and CEL (Comisión Ejecutiva Hidroeléctrica del Río Lempa) has been used to determine the crustal structure and the quality factor Q. Additionally some seismological aspects at the Berlin geothermal field and neighbouring Lempa river are shown using the seismicity reported for the recent seismic network installed by CEL.

The quality factor Q under the volcanic belt in El Salvador was determined as a function of frequency in the range 1-16 Hz, using 553 microearthquakes with focal depths between 0-20 kms. The model developed by Aki and Chouet for the coda wave generation and propagation was used. The analysis was made for different groups of data. An average of all data results in a Q relationship of :

$$Q = 52f^{0.78}$$

where f is the frequency.

The crustal P and S-velocity structure in central El Salvador has been determined using simultaneous inversion for structure and hypocentral location using arrival times for 506 shallow earthquakes. The model determined was:

Depth (km)	P-velocity (km/sec)	S-velocity (km/sec)	Vp/Vs
0	3.36	2.06	1.63
1	4.72	2.59	1.82
5	6.06	3.52	1.72
11	6.54	3.80	1.72
25	6.97	4.05	1.72

The statistics show an increase of the seismicity since 1995 for the Lempa river area. Correlation between reinjection and seismicity was not found

for the Berlin geothermal field and a-value shows that geothermal production has little influence on the level of local seismicity.

The stress drop in the Geothermal field is smaller than the Lempa river area. The average observed values are 0.4 and 2.5 bars respectively. Differences for b values and Vp/Vs ratio were also observed. The focal mechanism at the injection zone suggest thrust faulting. In the volcanic structures east and south-east of Berlin the mechanisms do not show any consistent type although fault planes are dominantly in the NE-SW or NW-SE direction in agreement with the local observed surface faulting.

CRUSTAL STRUCTURE IN THE VOLCANIC CHAIN OF EL SALVADOR BY SIMULTANEOUS INVERSION OF P AND S WAVE DATA

Griselda Marroquín and Jens Havskov

ABSTRACT

The crustal P and S-velocity structure in central El Salvador has been determined using simultaneous inversion for structure and hypocentral location using arrival times for 506 shallow earthquakes. The Vp/Vs ratio was independently determined to be 1.72±0.08. The model determined was:

Depth (km)	P-velocity (km/sec)	S-velocity (km/sec)	Vp/Vs
0	3.36	2.06	1.63
1	4.72	2.59	1.82
5	6.06	3.52	1.72
11	6.54	3.80	1.72
25	6.97	4.05	1.72

This model has higher velocities than models for other areas in Central America.

INTRODUCTION

El Salvador is located on the western edge of the Caribbean plate, which interacts with four other lithospheric plates in the region of Central America. The principal features that affect El Salvador are the Middle America Trench, where the Cocos plate is subducted below the Caribbean plate and the resulting chain of Quaternary volcanoes that extends from Guatemala, through El Salvador and Nicaragua, to Costa Rica (Bommer et al., 1996). The bulk of seismic activity in Central America occurs on the interplate thrust zone, but a significant amount of seismic activity

concentrates along the volcanic chain (Harlow et al., 1993). Around 80% of the seismic activity in El Salvador has its origin in the subduction zone, while the other 20% is generated either by local fault movements or volcanic activity (Atakan and Torres, 1993). Harlow et al. (1993) show the location of modified Mercalli (MM) intensity damage from 22 upper-crustal earthquakes in western El Salvador since 1700; nine of these severely damaged the city of San Salvador. These earthquakes were moderate-size shallow-focus with magnitudes less than or equal to 6.6. Earthquakes of magnitude up to 7.9 occurring along the subduction zone have severely damaged San Salvador five times since 1700 (Harlow et al., 1993). The last event to damage San Salvador was in October 10, 1986. The hypocenter determined by Harlow et al. (1993) was made using a simplified version of the velocity structure found at Cascade Volcanoes and was used because of the lack of direct velocity measurements beneath San Salvador. Marroquín and Ciudad Real (1995) made a preliminary crustal structure model for San Salvador city using the method of minimum apparent velocity. Only structure up to 7 km depth was determined.

Thus the crustal structure beneath El Salvador is poorly known. A bibliography search was made and scientists involved in seismological research in the area were consulted about crustal structure studies. Apparently no other study than by Marroquín and Ciudad Real (1995) has been done.

In the rest of the Central American countries, a few other studies can be found. Matumoto et al. (1977), used seismic data from explosions and local earthquakes to determine shallow crustal structure near Managua, Nicaragua, and to derive a complete crustal model for northern Costa Rica. The method of minimum apparent velocity was used in the analysis. According to Matumoto et al. (1977), the total thickness of the crust beneath the central volcanic province of northern Costa Rica was about 43 km, a three layer crust was reported with velocities of 5.1, 6.2 and 6.6 km/sec with thicknesses of 8.2, 12.9 and 22.3 km, respectively and the upper mantle velocity was 7.9 km/sec.

Kim et al. (1982) used travel time and amplitude data of wide-angle reflections for the central portion of northern Central America and assuming a Pn velocity of 8.0 km/sec, derived P-wave velocities as 5.79, 6.14 and 6.80 km/sec and layer thicknesses of 9.6, 14.6 and 13.2 km. respectively. The total crustal thickness was estimated at 37.4 km.

Protti et al. (1996) have resolved the crustal and upper mantle velocity structure beneath central Costa Rica using P-wave arrival times. Thurber's (1983) iterative inversion method was used to simultaneously estimate velocities along a three-dimensional grid and hypocentral parameters of local earthquakes. They found low velocities (4.0 to 4.8 km/sec) in the shallow crust (above 10 km) near the active volcanoes and associated with a NW-SE trending late Cretaceous to late Tertiary sedimentary basin southeast of Herradura Peninsula. High velocities (5.4 to 5.7 km/sec) in the shallow crust correlate with outcrops of late Jurassic to early Tertiary ultramafic ophiolitic units and with basic Tertiary volcanic units. At depths between 20 and 30 km, high velocities (6.8 to 7.2 km/sec) were associated with the subducting Cocos plate under Costa Rica and two prominent low-velocity layers (6.3 to 6.5 km/sec) were present about 30 km trenchward of the volcanic arc and along the projection of the aseismic Cocos Ridge as it subducts beneath Costa Rica.

Ligorría and Molina (1997) determined the crustal velocity structure of southern Guatemala using the method of minimum apparent velocity and converted waves, and reported the Moho depth of 46 km and five layer crust with velocities of 5.0, 5.7, 6.0, 6.6 and 7.0 km/sec with thicknesses of 7, 7, 10, 7 and 15 km, respectively.

These models (Figure 5) are quite different and might not be appropriate for El Salvador. The purpose of this study is to use local earthquake arrival times to invert for the crustal structure in El Salvador.

METHOD

Following Kissling (1988) and Kissling et al. (1994), the arrival time of a seismic wave generated by an earthquake is a nonlinear function of the station coordinates, the hypocentral parameters (including origin time and geographic coordinates), and the velocity field. In general, neither the hypocentral parameters nor the velocity field are known. Thus the arrival time is the only measurable quantity. However, we may always make an educated guess for the unknown parameters. Using a simple averaging velocity model, we trace rays from the trial source location to the receivers and calculate theoretical arrival times. The differences between the observed and the calculated arrival time, the residual travel time, can be expanded as functions of the differences (Δ) between the estimated and the

true hypocentral and velocity parameters. To calculate suitable adjustments (corrections) to the hypocentral and model parameters, we need to know the dependence of the observed travel times on all parameters.

Following Crosson (1976) and Kissling et al. (1994), in an ensemble of arrival time observations for, say, q total events recorded at p stations, the arrival time for the ith event at the jth station is

$$T_{ij} = T_{ij} (h_{1i}, h_{2i}, h_{3i}, h_{4i}, m_1, ..., m_l) \quad (1)$$

Where h_{1i} ... are the hypocenter parameter and m_l ... are the aggregate of possible parameters describing the model. Applying a first-order Taylor series expansion to (1), we obtain a linear relationship between the travel time residual and adjustments to the hypocentral (Δh_{ki}) and velocity (Δm_k) parameters:

$$\Delta T_{ij} = \sum_{k=1,4} (\partial T_{ij} / \partial h_{ki}) \Delta h_{ki} + \sum_{k=1,l} (\partial T_{ij} / \partial m_k) \Delta m_k + e_{ij} \quad (2)$$

$$\Delta T_{ij} = T_{ij} - T_{ij}^0 \qquad \Delta h_{ki} = h_{ki} - h_{ki}^0 \qquad \Delta m_k = m_k - m_k^0$$

The quantities h_{ki}^0 and m_k^0 are points in hypocenter and model space where the partial derivatives are evaluated. Following the usual method, ΔT_{ij} is associated with O - C (observed minus calculated) residuals calculated by assuming an initial set of solution parameters.

In matrix notation, the coupled hypocenter velocity model parameter relation (2) can be written as (Kissling et al., 1994).

$$t = Hh + Mm + e = Ad + e \quad (3)$$

t vector of travel time residuals;
H matrix of partial derivatives of travel time with respect to hypocentral parameters;
h vector of hypocentral parameter adjustments;
M matrix of partial derivatives of travel time with respect to velocity model parameters;
m vector of velocity model parameter adjustments;
e vector of travel time errors, including contributions from errors in measuring the observed travel times, errors in t_{cal} due to errors in station coordinates, use of the wrong velocity model and

hypocentral coordinates, and errors caused by the linear approximation;

A matrix of all partial derivatives;

d vector of hypocentral and model parameter adjustments.

To reduce the computational burden of solving the very large system of equation (3), Pavlis and Booker (1980) and Spencer and Gubbins (1980) independently introduced an algorithm, to separate A into the two smaller matrices, one containing the hypocenter location information, and one containing the velocity model parameter information (Kissling 1994). Neglecting the coupled inverse model problem while locating the earthquakes may only introduce systematic errors in the hypocenter locations as a result of error in the assumed velocity model or because a station distribution does not allow the precise location of the hypocenters in some specific areas (Kissling, 1988).

In the coupled inverted problem, the travel time data set is simultaneously inverted for the unknown parameters velocity model, hypocentral parameters and station corrections. Following Tarantola (1987), the solution of the linearized damped least-squared problem may be written as follows (Maurer and Kradolfer, 1996).

$$d = (A^T C_D^{-1} A + C_M^{-1})^{-1} A^T C_D^{-1} t \qquad (4)$$

where

d= model adjustments;

t= travel time residuals;

A= jacobian matrix;

C_D = data covariance matrix; and

C_M = model covariance matrix.

The diagonal elements of C_D contain the data variances, and the off-diagonal elements are mostly equal to zero. C_D allows the individual data points to be weighted, and further more, it removes the dimensionality of the input data. The model covariances C_M represent how much the solution is allowed to differ from the initial model. These model covariances are based on a priori information. With increasing C_M^{-1}, the model adjustments d become smaller, and therefore, equation (4) is called the damped least squares solution. Like C_D, the operator C_M also removes the dimensionality of the model parameters (Maurer and Kradolfer, 1996).

The solution of the coupled inverse problem has been implemented in the computer program VELEST. This program simultaneously locate earthquakes and calculate 1-D (layered) velocity models with station corrections. The forward problem is solved by ray tracing from source to receiver, computing the direct, refracted, and (optionally) the reflected rays passing through the 1-D model. The inverse problem is solved by full inversion of the damped least squares matrix [AtA + Λ] (A= Jacobi matrix, At= transposed Jacobi matrix; Λ=damping matrix). Because the inverse problem is non-linear, the solution is obtained iteratively, where one iteration consists of solving both the complete forward problem and the complete inverse problem once (Kissling, 1995).

DATA SELECTION

One of the most important steps for any inversion of local earthquake data is the selection of the data for quality and for geometrical distribution (Kissling, 1988).

The data for this study was recorded at two digital seismic networks (Figure 1). One is operated for CIG (Centro de Investigaciones Geotécnicas) and the another for CEL (Comisión Ejecutiva Hidroeléctrica del Río Lempa). For CIG, the information was selected from 01/1992 to 08/1997 and for CEL from 07/96 to 06/97. The criteria for selecting an event was that it was recorded on at least 4 stations, had maximum RMS of 0.5 sec and maximum gap of 180 degrees. The data selected consisted of 506 events located along the volcanic chain (Figure 1) with focal depths between 0 to 20 km. The total number of readings was 5685. In El Salvador, the majority of events occur along the shallow subduction zone. These events were not used in the inversion since all events were outside the network and therefore provided poor constraint on the inversion. In addition, it is expected that the structure is more inhomogeneous between the subduction zone and the volcanic chain than along the volcanic chain. Deep well located earthquakes just below the volcanic chain were very few and were therefore not used. This means that the data set cannot resolve the structure in the deeper crust.

DATA ANALYSIS

Inversion for crustal structure is very sensitive for choice of initial model. In general, crustal structure inversion requires many tests to find the best initial model (Kissling, 1994). For El Salvador, it would be natural to choose an initial model from either Guatemala or Nicaragua, however that in itself would mean limiting the initial choice. For El Salvador it was therefore decided to try to get a model from scratch without using information from neighbouring countries, and then compare the results with the neighbouring countries models.

Since the inversion does not resolve layer thickness, the first initial models were chosen to have 40 layers with a linear increasing velocity. After the inversion, several layers have the same velocity and in that way, one gets an indication of the layer boundaries.

The data set used has both P and S-waves. Obviously the P-times are the most accurate, however by using the S-arrivals, the hypocentral location is more accurate. The preselection of the data also establishes that only high quality data is used. The inversion program inverts for P and S-velocity and a Vp/Vs velocity ratio has to be given for calculate the initial S-velocity model which is taken from the initial P-velocity model. Thus only p-velocity start models are used. The Vp/Vs ratio was determined to 1.72 $\pm$ 0.08 by taking the averages Vp/Vs calculated with a Wadati diagram individually for 94 events. Only events with at least 5 pairs of P and S-times, a maximum Wadati fit of 0.4 sec RMS and a correlation coefficient of at least 0.7 were used.

The first step was then to use 3 gradient multilayer models (Figure 2) with start velocities in the first layer of 4.5, 5.5 and 6.0 km/sec for model 1, 2 and 3, respectively. The reason to chose such different start models was to investigate whether is was possible to arrive at a unique model from different starting models and in that way get some assurance that a best fit model was obtained. The results are seen on Figure 2. As it can be seen both the lowest and highest velocity models converge toward a similar model which is closest to the middle velocity starting model. This is reassuring since it shows that our data can resolve gross velocity structures. It is also seen that the final structure is obtained after about 10 iterations so there is no need to do more than 10-15 iterations. The initial RMS was lowest for model 2 while the final RMS was 0.2228, 0.2266 and 0.2266 for the 3 models respectively. The 3 final models can hardly be

distinguished by the RMS, but of course they are also very similar. The variation between the 3 final models might indicate the uncertainly of the inversion.

The next step was to simplify the 3 final models by selecting fewer layers. A simplified average model with 7 layers is shown in Figure 3. A new inversion was now made with this model (model 4) as starting model. This showed little variation in the start and final models, which was obtained after 5 iterations. The RMS of fit was 0.2227. Considering what details normally are available about the crustal velocities, model 4 might still be too detailed and a further simplification was made by joining layers 4 and 5, and 6 and 7. This model 5 was then again used as input for inversion and the result is shown in Figure 4. There was now very little variation between initial and final model and after 2 iterations the changes were insignificant. The RMS was 0.2195. The model 5 is considered as the final result for this study (Table 1). The S-velocity model is very close to the P-velocity model, and it is sufficient to just use the P-velocity model and a Vp/Vs ratio of 1.72.

VELEST can optionally also find low velocity layers and if set to not allow low velocity layers, warning will be given if the program would have come out with low velocity layers. The low velocity layer option was tested since there were many warnings about possible low velocity layers. However, the low velocity layers were very thin with high velocity contrasts and the whole inversion became more unstable, so no attempt was made to determine a model with low velocity layers. It is not unreasonable that low velocities should be present since they are found in Costa Rica (Protti et al., 1996), however it does not seem possible to resolve with the current data set.

Table 2 shows a list of stations and station corrections obtained. In general, the station corrections are for the majority less than 0.1 sec for P and 0.3 for S and therefore insignificant both in terms of earthquake locations and for the inversion. As a test, the final model was also used as input to an inversion without calculating station corrections. However, the results were nearly identical to model 5, as expected from the station corrections (Figure 4).

In order to test whether lateral changes could be distinguished between Ilopango and Berlin data, two subsets of data were selected (Figure 1). Both consist of a concentrated set of well located shallow events that are spatially separated. CEL had 77 events of which all but 3 had depths less

than 5 km and Ilopango lake data set consisted of 164 events with depths up to 11 km. The inversion was done to get the structure above 6 km depth assuming that the velocity below 6 km depth was the same as for the general model. Initially, the same procedure as used for the whole data set was attempted, with gradient type starting models with layer thickness of 1 km. However it was not possible to get any consistent results since each start model would give different results but closely tied to the start model. Clearly the resolution power of the data was much poorer in this case as compared to the whole data set. From the general model it seems that the first 6 km of the crust can be approximated by a two layer model of thickness of 1 and 5 km (Figure 4). In order to simplify, 25 two layer models over half space were tested for the two areas. Table 3 shows the 4 models with smallest RMS.

DISCUSSION

In this study it seems that the data set is well able to resolve the crustal structure down to 25 km depth.

The crustal structure for this study is compared with structures in neighbouring countries (Matumoto et al., 1977; Kim et al., 1982; Ligorría and Molina, 1997). Our results show consistently higher velocities than the other models except for depths less than 5 km (Figure 5). The velocity in the first and second layer is near to the value reported by Matumoto et al. (1977) near Managua, Nicaragua. The layer third velocity is near the value reported by Marroquín and Ciudad Real (1995) for San Salvador City (Figure 5).

Considering the significant differences in the Central American models, a test was made to relocate the 506 events with Hypocenter (Lienert and Havskov, 1995) using the new El Salvador model and the model by Matumoto et al. (1977) and Ligorria and Molina (1997). The average travel time residual RMS for all events for the models were 0.239, 0.252 and 0.262 sec respectively. It thus seems that the new model from this study is more appropriate for El Salvador than the other 2 models.
The attempt to compare the structure for 2 different areas does not reveal significant differences and the results are in general uncertain. The Ilopango lake area seems to be close to the "normal model", while the best

model for the geothermal field has lower velocity in the first layer(2.25 vs 3.36 km/sec) than the "normal model".

As a final test for the reliability of the inversion, the models of L-M and MAT were used as input models for the data set. In both cases, the inversion gave final models near the final model found for this study. This is evidence, that the final model is reliable.

REFERENCES

Atakan, K. and R. Torres (1993). Local Site Response in San Salvador, El Salvador Based on the October 10, 1986 Earthquake. Reduction of Natural Disasters in Central America, Report No. 6. Institute of Solid Earth Physics, University of Bergen, Norway.

Bommer, J.J, D. A. Hernandez, J. A. Navarrete and W. M. Salazar (1996). Seimic hazard assessments for El Salvador. Geofisica Internacional, Vol. 35, Num. 3, 227-244.

Crosson, R. S. (1976). Crustal Structure Modeling of Earthquake Data 1. Simultaneous Least Square Estimation of Hypocenter and Velocity Parameters. J. Geophys. Res., 81, 3036-3046.

Harlow, D. H., R. A. White, M. J. Rymer and S. Alvarez. (1993). The San Salvador Earthquake of 10 October 1986 and its Historical Context. Bull. Seism. Soc. Am., 83, 4, 1143-1154.

Havskov, J. (1997). The Seisan Earthquake Analysis Software for the IBM PC and SUN. Version 6.0. Institute of Solid Earth Physics, University of Bergen, Norway.

Kim, J. J., T. Matumoto and G. V. Latham (1982). A Crustal Section of Northern Central America as Inferred from Wide-Angle Reflections from Shallow Earthquakes. Bull. Seism. Soc. Am. 72, 925-940.

Kissling, E. (1995). Program VELEST USER'S GUIDE - Short Introduction. Second draft version 5th October 1995. Institute of Geophysics, ETH Zuerich.

Kissling, E., S. Solarino and M. Cattaneo (1995). Improved Seismic Velocity Reference Model from Local Earthquake Data in Northwestern Italy. Terra Nova, 7, 528-534.

Kissling, E., W. L. Ellsworth, D. Eberhart- Phillips and U. Kradolfer (1994). Initial reference models in local earthquake tomography. J. Geophys. Res. 99, 19635-19646.

Kissling, E. (1988). Geotomography with Local Earthquake Data. Rev. of Geophysics, 26, 659-698.

Lienert, B. R. E. and J. Havskov (1995). A computer program for locating earthquake both locally and globally, Seismological Research Letters, 66, 26-36.

Ligorria, J. P. and E. Molina (1997). Crustal velocity structure of southern Guatemala using refracted and Sp converted waves. Geofísica Internacional, 36, 9-19.

Marroquín, G. and M. Ciudad Real (1995). Modelo de Corteza Preliminar para el Area Metropolitana de San Salvador y sus Alrededores, Utilizando Sismicidad Natural. Centro de Investigaciones Geotécnicas, Ministerio de Obras Públicas.

Matumoto, T., M. Ohtake, G. Latham and J. Umana (1977). Crustal Structure in Southern Central America. Bull. Seism. Soc. Am. 67, 121-134.

Maurer, H. and U. Kradolfer (1996). Hypocentral Parameters and Velocity Estimation in the Western Swiss Alps by Simultaneous Inversion of P- and S. Wave Data. Bull. Seism. Soc. Am. 86, 32-42.

Pavlis, G. L. and J. R. Booker (1980). The Mixed Discrete- Continuous Inverse Problem: Application to the Simultaneous Determination of

Earthquakes Hypocenters and Velocity Structure. J. Geophys. Res. 85, 4801-4810.

Protti, M., S. Y. Schwartz, and G. Zandt (1996). Simultaneous Inversion for Earthquake Location and Velocity Structure Beneath Central Costa Rica. Bull. Seism. Soc. Am. 86, 19-31.

Spencer, C. and D. Gubbins (1980). Travel-time inversion for simultaneous earthquake location and velocity structure determination in laterally varying media. Geophys. J. R. astr. Soc., 63, 95-116.

Tarantola , A. (1987). Inverse Problem Theory. Elsevier, Amsterdam.

Thurber, C. H. (1983). Earthquake Locations and Three-Dimensional Crustal Structure in the Coyote Lake Area, Central California. J. Geophys. Res. 88, 8226-8236.

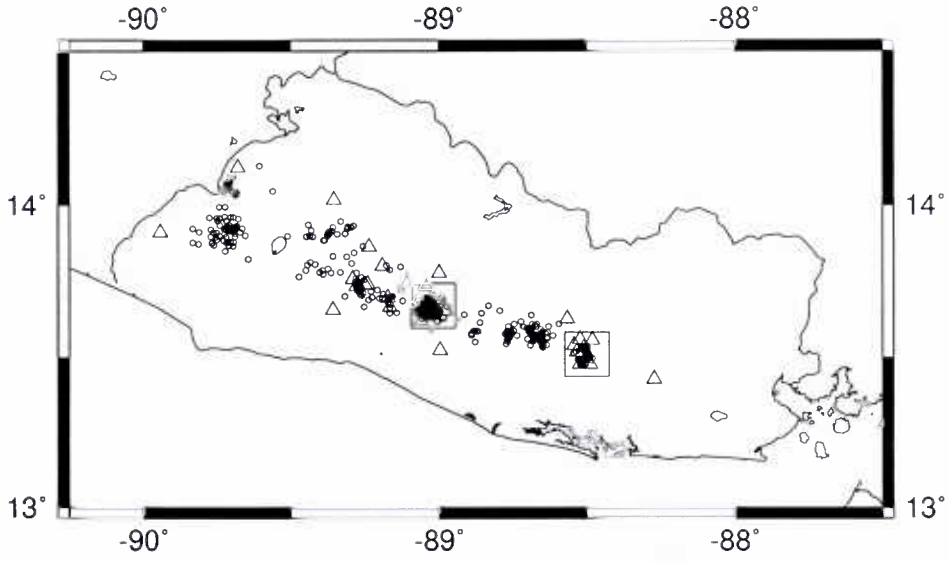

Figure 1: Epicenters (circle) and stations (triangle) used for the inversion.
The squares are selected areas for partial inversion. CEL stations are located between longitude 88.57° W and 88.47° W, the other stations are from CIG network.

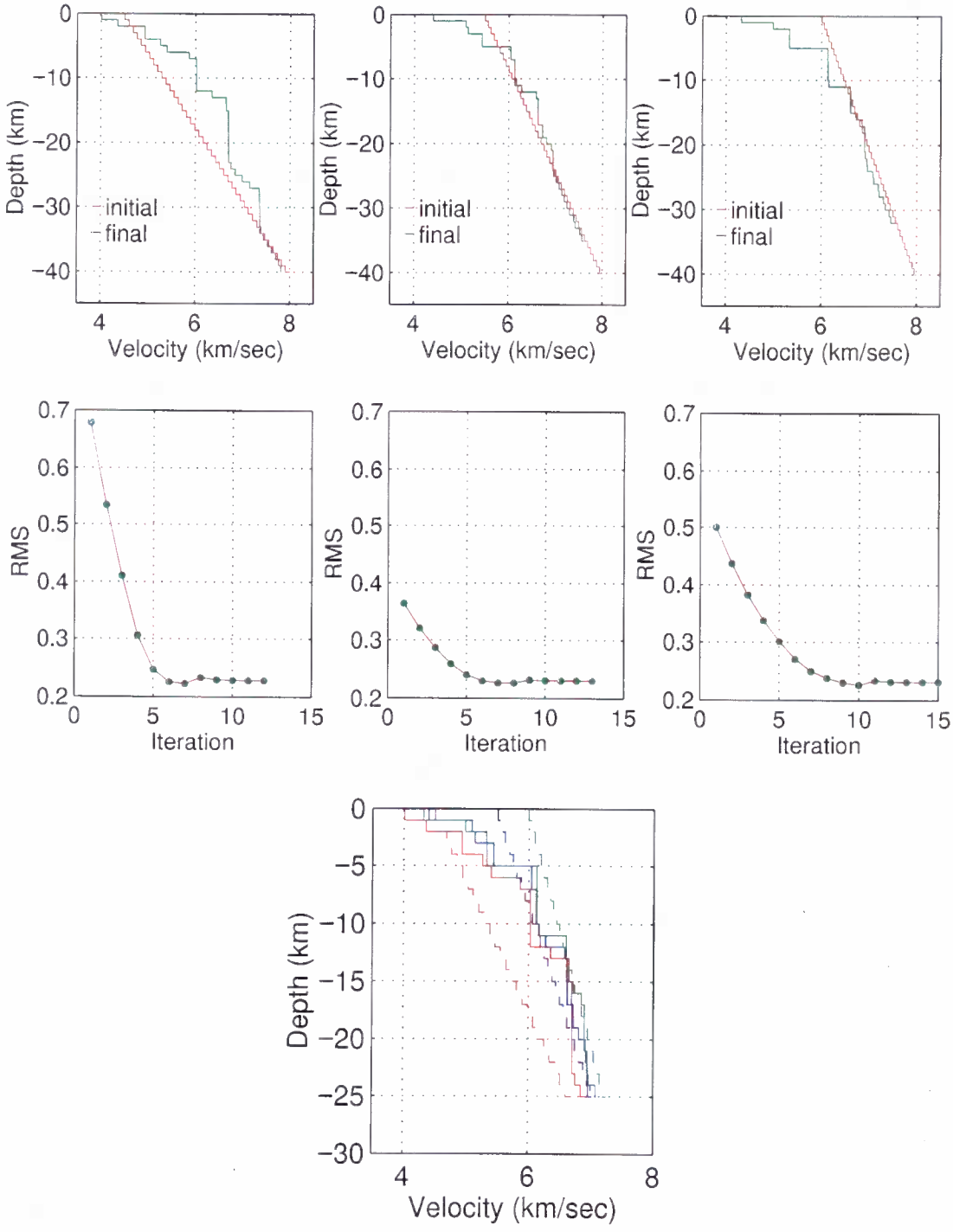

Figure 2: Gradient layer starting models and the models given by the inversion.
The middle figures show the RMS as a function of iteration number for each model. The bottom figure is a superposition of the 3 models of figures on top.

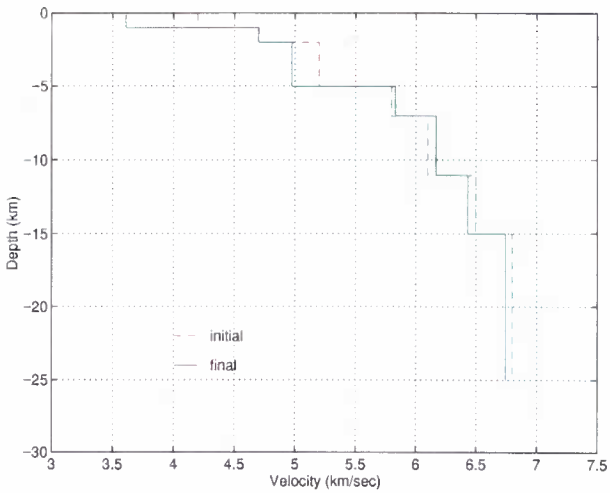

Figure 3: Average model from Figure 2 (dashed line), used as input model for a new inversion, the result is shown with continuous line.

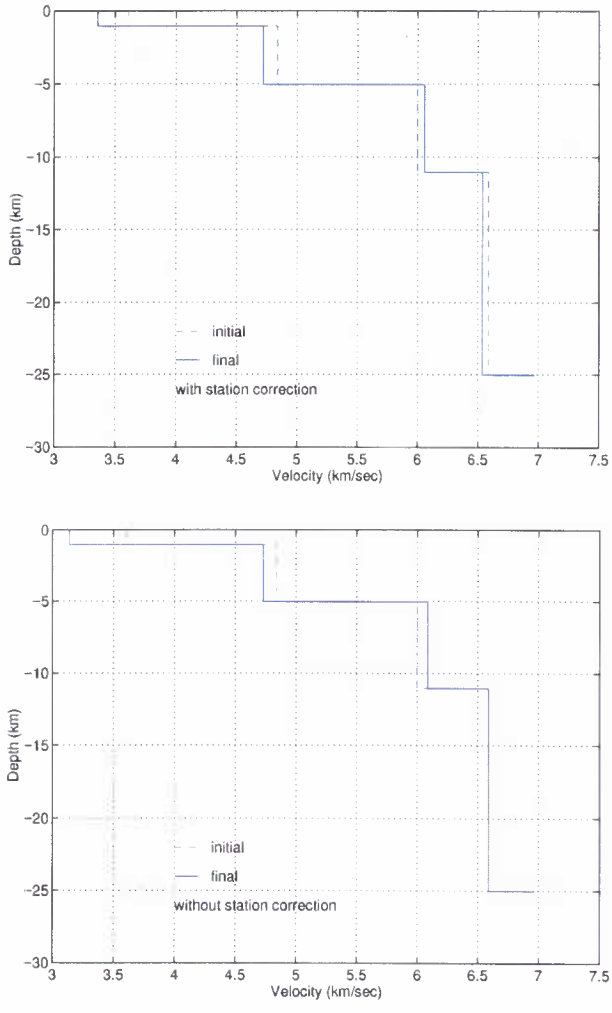

Figure 4: Final inversion.
The input model (dashed line) is from Figure 3 where layers 2-3, 4-5 and 6-7 were averaged in order to simplify the model. The top figure shows results when using station correction and bottom figure the results without using station correction. The velocity in the half space was fixed to 6.97 km/sec.

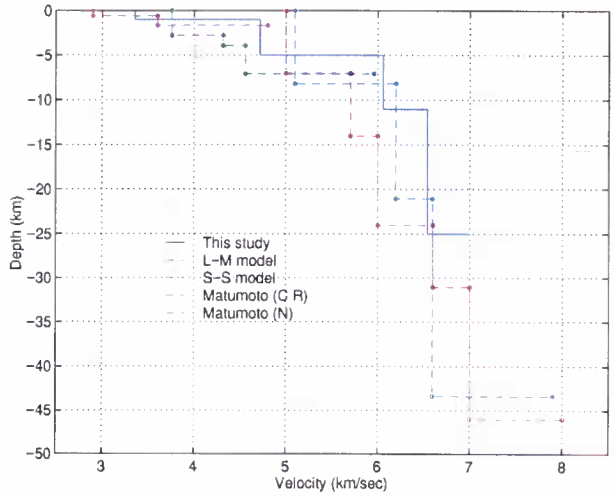

Figure 5: Comparison with other models in neighbouring contries.
L-M model is Ligorria and Molina (1997) for southern Guatemala, S-S model is for San Salvador (Marroquin and Ciudad Real, 1995), Matumoto (C R) and (N) are models for Costa Rica and Nicaragua (Matumoto et al., 1977).

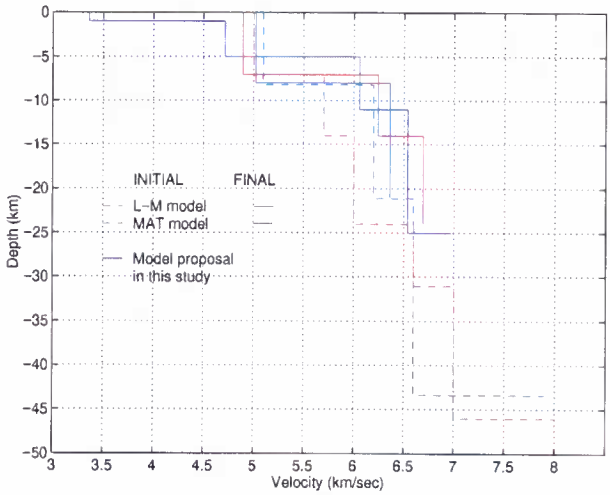

Figure 6: Using another input models.
The L-M model (Ligorria and Molina, 1997) and MAT model (Matumoto et al., 1977) were the input models for the inversion (dash lines) , the continuous lines are the inversion output using our data set.

Table 1: Proposal model for the volcanic chain of El Salvador.

Depth (km)	P-velocity (km/sec)	S-velocity (km/sec)	Vp/Vs
0	3.36	2.06	1.63
1	4.72	2.59	1.82
5	6.06	3.52	1.72
11	6.54	3.80	1.72
25	6.97	4.05	1.72

Table 2: Stations coordinates and station corrections.

Station	Latitude North	Longitude West	Elevation (meters)	Number of P-wave readings for inversion	Station correction for P-wave (secs.)	Number of S-wave readings for inversion	Station correction for S-wave (secs.)
	CIG network						
CUS	13°54.55'	89°56.65'	677	83	-0.052	41	0.127
LFU	13°44.92'	89°06.83'	732	230	-0.019	111	-0.152
QZA	13°31.43'	88°59.82'	250	190	-0.020	157	-0.355
SJA	13°40.00'	89°10.00'	1100	71	-0.126	43	-0.185
TME	14°01.02'	89°21.33'	516	265	-0.073	150	-0.188
YPE	14°07.30'	89°40.83'	1581	148	-0.103	89	-0.040
VSS	13°44.50'	89°14.50'	1250	51	0.315	26	0.439
VSM	13°25.68'	88°16.45'	2129	25	0.010	10	0.103
SJA1	13°40.00'	89°10.00'	1100	70	-0.169	32	-0.257
HUE2	13°46.70'	89°00.00'	910	36	-0.171	10	-0.628
ANG3	13°48.00'	89°11.50'	850	124	0.028	70	-0.214
OJO4	13°51.80'	89°14.20'	645	56	-0.117	19	-0.216
ADE5	13°39.50'	89°21.50'	1200	90	0.037	37	0.253
LFR1	13°37.40'	89°03.70'	1000	297	-0.067	182	-0.075
LCB2	13°39.30'	88°58.70'	710	319	-0.040	187	-0.088
LBR3	13°44.30'	89°02.60'	770	240	-0.014	135	0.013
PIC4	13°44.36'	89°15.30'	1960	125	0.094	47	0.458
GRD5	13°45.50'	89°17.50'	1520	115	-0.067	49	-0.342
BOQ6	13°44.10'	89°16.80'	1830	145	0.000	55	0.082
CIG	13°41.88'	89°10.40'	616	5	0.383	6	0.095
	CEL network						
LPA	13°28.68'	88°32.12'	1528	82	0.061	37	0.550
TCP	13°29.34'	88°30.42'	1594	135	-0.010	75	0.067
MUM	13°33.33'	88°28.75'	410	97	0.227	83	0.454
SDM	13°28.43'	88°29.08'	900	108	0.036	66	-0.010
SJU	13°31.20'	88°32.01'	1024	140	0.089	36	0.183
MTA	13°31.20'	88°30.72'	480	115	0.060	112	0.068
LAL	13°32.36'	88°32.53'	474	139	0.143	96	0.223
SAN	13°33.46'	88°31.37'	310	120	0.095	65	0.137
LGU	13°38.68'	88°33.68'	220	21	0.016	17	0.165

Table 3: Inversion for Ilopango lake and Berlin geothermal field

BERLIN GEOTHERMAL FIELD		input		output		iteration
layer	depth (km)	velocity (km/sec)	RMS (sec)	velocity (km/sec)	RMS (sec)	number
1	0	2.0	0.2277	2.25	0.0893	10
2	1	4.5		4.68		
3	5	6.0		6.00		
1	0	3.5	0.1900	3.59	0.0935	10
2	1	4.0		4.58		
3	5	6.0		6.00		
1	0	3.5	0.1262	3.67	0.0930	10
2	1	5.0		5.42		
3	5	6.0		6.00		
1	0	4.5	0.1495	3.94	0.0936	10
2	1	5.5		5.85		
3	5	6.0		6.00		

ILOPANGO LAKE		input		output		iteration
layer	depth (km)	velocity (km/sec)	RMS (sec)	velocity (km/sec)	RMS (sec)	number
1	0	2.0	0.3144	2.27	0.2015	3
2	1	4.5		4.93		
3	5	6.0		6.00		
1	0	3.5	0.2868	3.83	0.1942	10
2	1	4.0		4.86		
3	5	6.0		6.00		
1	0	3.5	0.2716	3.79	0.2005	10
2	1	5.0		5.38		
3	5	6.0		6.00		
1	0	4.5	0.2949	4.72	0.1962	10
2	1	5.5		5.90		
3	5	6.0		6.00		